J|A|C|S
ARTICLES
Published on Web 01/07/2003

Structure of the Aqueous Solvated Electron from Resonance Raman Spectroscopy: Lessons from Isotopic Mixtures

Michael J. Tauber and Richard A. Mathies*

Contribution from the Department of Chemistry, University of California, Berkeley, California 94720

Received August 30, 2002; Revised Manuscript Received November 1, 2002; E-mail: rich@zinc.cchem.berkeley.edu

Abstract: The structure and thermodynamics of the hydrated electron are probed with resonance Raman spectroscopy of isotopic mixtures of H_2O and D_2O. The strongly enhanced intramolecular bends of $e^-(H_2O)$ and $e^-(D_2O)$ produce single downshifted bands, whereas the e^-(HOD) bend consists of two components: one slightly upshifted from the 1446 cm^{-1} bulk frequency to 1457 cm^{-1} and the other strongly downshifted to ~1396 cm^{-1}. This 60 cm^{-1} split and the 200 (120) cm^{-1} downshifts of the OH (OD) stretch frequencies relative to bulk water reveal that the water molecules that are Franck−Condon coupled to the electron are in an asymmetric environment, with one proton forming a strong hydrogen bond to the electron. The downshifted bend and librational frequencies also indicate significantly weakened torsional restoring forces on the water molecules of e^-(aq), which suggests that the outlying proton is a poor hydrogen bond donor to the surrounding solvent. A 1.6-fold thermodynamic preference of the electron for H_2O is observed based on the relative intensities of the $e^-(H_2O)$ and $e^-(D_2O)$ bands in a 50:50 isotopic mixture. This equilibrium isotope effect is consistent with the downshifted vibrational frequencies and a relative reduction of the zero-point energy of H_2O bound to the electron. Our results enhance the cavity model of the solvated electron and support only those models that contain *water* monomers as opposed to other molecular species.

1. Introduction

After its identification in 1962,[1] the solvated electron in liquid water was found to be a ubiquitous species in aqueous radiation chemistry and a common product of the UV photolysis of many inorganic and aromatic molecules. Much information on the production,[2] reactivity,[3] dynamics,[4,5] and thermodynamics[6] of the hydrated electron has emerged over the years, but a structural understanding of this species has remained elusive. Besides intrinsic interest in determining the structural motifs in the hydration of an electron, this knowledge is fundamental to understanding the properties of this basic solute−solvent system.

Early experimental evidence on the structure of the aqueous solvated electron was provided by electron spin−echo envelope modulation (ESEEM) of electrons in aqueous glasses at 77 K.[7,8] These studies suggested that the electron is surrounded by six bond-oriented water molecules in an octahedral configuration, with the nearest protons located 2.1 Å from the electron centroid. An improved understanding of the ESEEM technique later suggested that the electron spin−echo pattern could arise from just two protons of a single dipole-oriented water molecule, or alternatively from two bond-oriented waters nearest the electron.[9] Studies of electrons in liquid water by pulsed ESR yielded a *g* value that was significantly lower than that of a free electron, which was attributed to the overlap of the solvated electron with oxygen atomic orbitals.[10,11] However, experimental data on the *g* value as a function of temperature, isotope, and salt concentration did not lead to a structural model.[10,12]

Spectroscopic studies[13,14] as well as ab initio calculations[15,16] of small electron−water clusters provide insight into the short-range interactions that are relevant to the structure of the aqueous electron in bulk liquid water. Calculations of $e^- + 6H_2O$ and $e^- + 12H_2O$ emphasize that the most stable cluster geometries are those which form the maximum number of hydrogen bonds to oxygen or the excess electron.[15,16] In agreement with calculations, IR spectra of small water anion clusters support the interpretation of a strong electron−water H bond;[13] however, the most recent studies of anion clusters with 5−11 waters suggest a linear "chainlike" network.[17] An additional ambiguity is the open question of how long-range (polarization) effects modulate or modify the short range interactions. For electron solvation in the bulk liquid, both long- and short-range forces

(1) Hart, E. J.; Boag, J. W. *J. Am. Chem. Soc.* **1962**, *84*, 4090.
(2) Blandamer, M. J.; Fox, M. F. *Chem. Rev.* **1970**, *70*, 59.
(3) Buxton, G. V.; Greenstock, C. L.; Helman, W. P.; Ross, A. B. *J. Phys. Chem. Ref. Data* **1988**, *17*, 513.
(4) Yokoyama, K.; Silva, C.; Son, D. H.; Walhout, P. K.; Barbara, P. F. *J. Phys. Chem. A* **1998**, *102*, 6957.
(5) Schmidt, K. H.; Han, P.; Bartels, D. M. *J. Phys. Chem.* **1992**, *96*, 199.
(6) Han, P.; Bartels, D. M. *J. Phys. Chem.* **1991**, *95*, 5367.
(7) Schlick, S.; Narayana, P. A.; Kevan, L. *J. Chem. Phys.* **1976**, *64*, 3153.
(8) Feng, D.-F.; Kevan, L. *Chem. Rev.* **1980**, *80*, 1.
(9) Dikanov, S. A.; Tsvetkov, Y. D. *Electron Spin−Echo Envelope Modulation (ESEEM) Spectroscopy*; CRC Press: Boca Raton, FL, 1992.
(10) Jeevarajan, A. S.; Fessenden, R. W. *J. Phys. Chem.* **1989**, *93*, 3511.
(11) Shiraishi, H.; Ishigure, K.; Morokuma, K. *J. Chem. Phys.* **1988**, *88*, 4637.
(12) Veselov, A. V.; Fessenden, R. W. *J. Phys. Chem.* **1993**, *97*, 3497.
(13) Bailey, C. G.; Kim, J.; Johnson, M. A. *J. Phys. Chem.* **1996**, *100*, 16782.
(14) Ayotte, P.; Johnson, M. A. *J. Chem. Phys.* **1997**, *106*, 811.
(15) Suh, S. B.; Lee, H. M.; Kim, J.; Lee, J. Y.; Kim, K. S. *J. Chem. Phys.* **2000**, *113*, 5273.
(16) Kim, J.; Park, J. M.; Oh, K. S.; Lee, J. Y.; Lee, S.; Kim, K. S. *J. Chem. Phys.* **1997**, *106*, 10207.
(17) Ayotte, P.; Weddle, G. H.; Bailey, C. G.; Johnson, M. A.; Vila, F.; Jordan, K. D. *J. Chem. Phys.* **1999**, *110*, 6268.

10.1021/ja021134a CCC: $25.00

are very important, as recognized by Newton in his early self-consistent field calculations which included a dielectric continuum.[18]

The most definitive prediction of the solvated electron structure in liquid water has been provided by molecular dynamics (MD) simulations.[19] A model that captures the main features of the experimental absorption spectrum, as well as most aspects of the femtosecond transient absorption spectroscopy,[20] is shown to have a most probable distribution of water molecules in the first solvent shell that is bond oriented and octahedral, with nearest protons and oxygen atoms respectively ~2.3 and 3.3 Å from the electron center,[19] in close agreement with the ESEEM results in the aqueous glass.

The lack of *experimental* data relevant to the solvated electron structure in the liquid phase provided strong motivation for our resonance Raman and fluorescence studies of the solvated electron in water.[21,22] We and Tahara[23] found frequency shifts and $>10^5$ resonance Raman enhancement of solvent modes from the solvated electron, and these findings illuminate the remarkably strong solvent−solute coupling of this system. With an awareness that resonance Raman studies of isotopically mixed systems have yielded critical insights into the structures of biological chromophores,[24,25] we decided to explore resonance Raman spectra of electrons solvated in mixtures of H_2O and D_2O. The spectra presented here reveal that water molecules are asymmetrically bound to the electron and that the binding occurs preferentially through hydrogen rather than deuterium. Our results are consistent with the traditional cavity model of the solvated electron but also provide an enhanced molecular picture of the electron−water "complex" which is found to have a very different hydrogen bonding pattern compared with that of bulk liquid water.

II. Materials and Methods

Our experimental procedures have been described earlier,[21,22] so we will detail only the changes and improvements. H_2O (Millipore/MilliQ), 99.9% D_2O (Cambridge Isotopes), or the 1:1, 2:1, 5.83:1 (mol/mol) mixtures of the isotopes contained 1.80 mM potassium ferrocyanide. The open flowing jet employed for Raman experiments had a thickness of ~100 μm. Photolysis (218 nm, ~160 μJ) and probe (683 nm, ~100 μJ) pulses of 5−10 ns duration were separated by 20 ns. The extinction coefficient of $Fe(CN)_6^{4-}$ at 218 nm was found to be identical in pure H_2O and D_2O (23 200 M^{-1} cm^{-1}). The photolysis-induced change of 683 nm transmission through the jet was measured with a pyroelectric power head (Molectron) to determine the concentration of electrons.

The collection optics were significantly changed from our previous reports. A backscattering geometry (135°) was employed, and the scattered light was collected with a Mitutoyo M-Plan NIR 10× microscope objective (NA = 0.26, f.l. 20 mm) designed for the visible−NIR spectral range. A 683 nm notch filter (Kaiser "SuperNotchPlus") located after the objective was angle tuned 8° from normal to acquire spectral data close to the Rayleigh line. For polarized spectra, a microfabricated vis−NIR wire-grid polarizer (Meadowlark Optics) was located after the notch filter. A quartz polarization scrambler was employed for measurements of both polarized and unpolarized spectra.

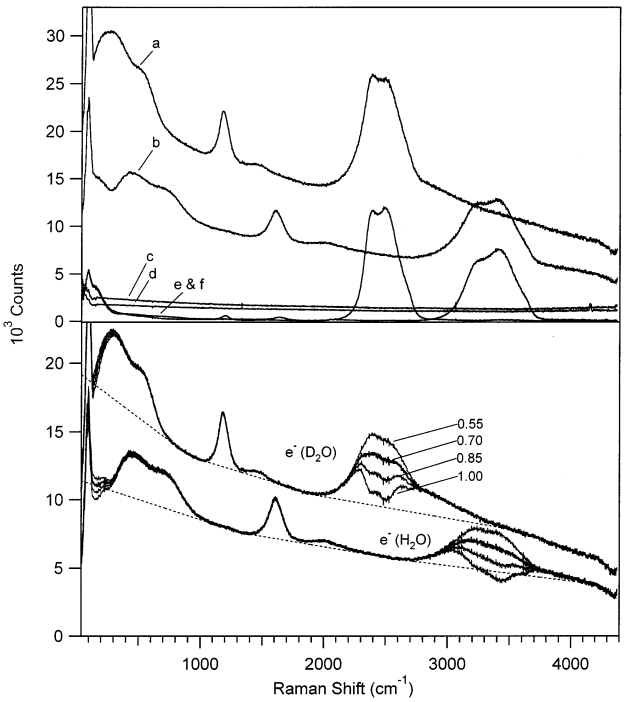

Figure 1. (Upper panel) Pump + probe spectra of 1.80 mM potassium ferrocyanide in D_2O (a) and H_2O (b). Pump-only spectra for the H_2O solution (c) and D_2O (d). Probe-only spectra are presented as e and f, respectively. (Lower panel) Solvated electron spectra resulting from the difference (pump + probe)−(pump-only) − K*(probe only). The $e^-(D_2O)$ spectrum is normalized to account for the different concentration−length values which are 8.0 and 9.4 μM cm for electrons in H_2O and D_2O, respectively. The maximum subtraction of the probe-only spectra which does not result in a subtraction anomaly in the OH/OD stretch region is K = 0.70. Interpolated baseline fits to the lowest points of the Raman spectra are shown as dashed lines. The emission below these baselines is due to fluorescence from the solvated electrons.[21]

Last, a near-IR doublet achromat (f.l. 50 mm) focused the collimated light onto the entrance slit of a 0.5 m F/4 spectrograph (Spex 500 M). The overall magnification of the system was kept low (50/20 = 2.5), since the width of the rectangular probe on the sample was ~100 μm and the entrance slit width was set at 200 μm. The 300 gr/mm grating employed here yields a spectral bandwidth of 1.33 nm (~21 cm^{-1} at 800 nm). The detector is a 1024 × 256 pixel front-illuminated LN_2 cooled open-electrode CCD (Roper LN/CCD-1024-E/OP/1). All polarized and unpolarized spectra were corrected for the instrument response using a calibrated 200 W lamp (Oriel QTH 63355).

Figure 1 presents an example of the data reduction procedure for the H_2O and D_2O spectra of the solvated electron. Initially, a probe-only background which includes minor stray laser lines (not shown) is subtracted from the pump + probe spectra a and b and from the probe-only spectra e and f. Each spectrum is divided by the instrument response. Full spectra result from the concatenation of two windows of the spectrograph, which are scaled by <10% to allow an exact match of the fluorescence and/or OD stretch (~broad 2400 cm^{-1} band) of the pump + probe and probe-only spectra. After concatenation, the nearly flat pump-only spectra c and d are fit by interpolation (Igor Pro, WaveMetrics) and then subtracted from the pump + probe spectra.

The subtraction of the probe-only spectrum is shown in Figure 1 (lower). Only the lowest frequency region (100−300 cm^{-1}) and the OH stretch region of the difference spectra depend on the scaling of the subtraction. The dominant effect of the solvated electron on the Raman scattering from the bulk ferrocyanide solution is due to the internal filter attenuation of the 683 nm probe, which is near the peak of the electron's absorption spectrum. A scalar attenuation of the probe-

(18) Newton, M. D. *J. Phys. Chem.* **1975**, *79*, 2795.
(19) Rossky, P. J.; Schnitker, J. *J. Phys. Chem.* **1988**, *92*, 4277.
(20) Schwartz, B. J.; Rossky, P. J. *J. Chem. Phys.* **1994**, *101*, 6917.
(21) Tauber, M. J.; Mathies, R. A. *J. Phys. Chem. A* **2001**, *105*, 10952.
(22) Tauber, M. J.; Mathies, R. A. *Chem. Phys. Lett.* **2002**, *354*, 518.
(23) Mizuno, M.; Tahara, T. *J. Phys. Chem. A* **2001**, *105*, 8823.
(24) Kurtz, D. M.; Shriver, D. F.; Klotz, I. M. *J. Am. Chem. Soc.* **1976**, *98*, 5033.
(25) Hildebrandt, P.; Stockburger, M. *Biochemistry* **1984**, *23*, 5539.

only spectrum compensates for this achromatic absorption.[26] The choice of attenuation factor is guided by the shape of the subtracted result in the OH and OD stretch region for a variety of unpolarized and polarized aqueous electron spectra. A factor as close to unity as possible is selected such that the resultant solvated electron spectra are without an anomalous dip because of subtraction of the OD/OH stretch of the bulk. The value of 0.70 meets these criteria. Further support for this factor is provided by the measured transmission of the 683 probe, which is 70 ± 5% for the experiments reported here.

The relative resonance Raman cross sections of the electrons in 100% H_2O and D_2O are important for accurate comparison and analysis of the isotopically mixed solutions. This result in turn depends on the relative quantum yield of electrons from ferrocyanide in the two solutions. Spectra were acquired in a single session with an alternation of H_2O and D_2O solutions to compensate for drifts in laser power (~3%) and the jet flow.[27] The thickness of the H_2O and D_2O jets monitored by the absorption of the 218 nm pump were found to differ <5%. A larger correction included in the scaling of the solvated electron spectra of Figure 1 is a 10−15% higher average concentration of electrons in D_2O, monitored by the change in probe absorption due to the pump and adjusted for the different 683 nm molar extinction coefficients of the solvated electron in D_2O (19 800 M^{-1} cm^{-1}) and H_2O (18 500 M^{-1} cm^{-1}).[28] This result indicates that the quantum yield of electron production from ferrocyanide monitored at a 20 ns delay is significantly higher in D_2O as compared with H_2O. A similar effect has been measured in ultrafast studies of the photolytic generation of electrons from I^- but has not been reported for ferrocyanide.[29]

III. Results

Figure 1 (lower) compares spectra of solvated electrons in the isotopically pure solvents. The isotope dependence of the fluorescence across the spectral window of Figure 1 shows that the fluorescence quantum yield of $e^-(D_2O)$ is 1.60 ± 10%-fold greater than that of $e^-(H_2O)$ at an equivalent concentration. Integration of the resonance Raman water bend yields a 1.04 ± 10% relative cross sectional ratio of $e^-(H_2O)/e^-(D_2O)$, with the error determined by the variability in the baseline fit. The ratio of Raman cross sections is significantly smaller than our previous experimental determination[22] of 1.6 ± 0.2 and is considered more accurate, given the care taken here in alternating samples.

Figure 2 presents a magnified view of the $e^-(H_2O)$ and $e^-(D_2O)$ spectra in the low-frequency and bend regions. The $e^-(H_2O)$ spectrum can be accurately fit with four Gaussian peaks at 225, 410, 530, and 698 cm^{-1}. The three peaks at highest frequency are identified as water librations.[30] The peak at 225 cm^{-1} coincides with a low-frequency peak identified previously and assigned tentatively as the overtone of a hindered translation.[22] The fit to $e^-(D_2O)$ includes a fixed component at the low-frequency translational assignment of 220 cm^{-1} and yields optimized components centered at 320 and 540 cm^{-1}, which correlate to the 530 and 698 cm^{-1} librations of $e^-(H_2O)$. A librational peak intermediate to the 320 and 540 cm^{-1} bands is not observable in our $e^-(D_2O)$ spectra nor is one discernible in fits to the off-resonance Raman spectra of pure D_2O.[30]

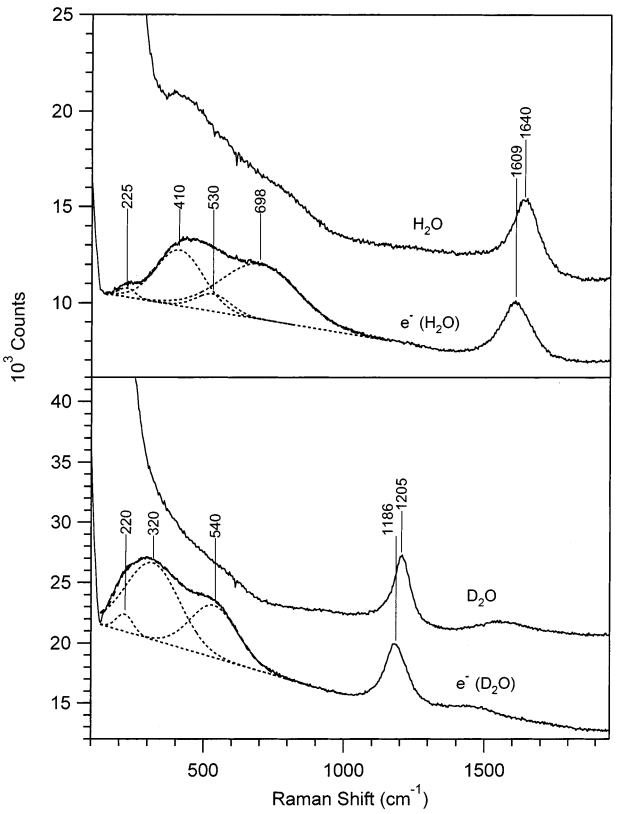

Figure 2. H_2O (upper panel) and D_2O (lower panel) low-frequency spectra of the solvated electron, compared with spectra of the pure solvent scaled to approximately equal bend intensity. The four-peak Gaussian fit to $e^-(H_2O)$ was optimized with a free variation of peak positions, widths, and heights. The resultant fit is indistinguishable from the actual spectrum. A three-peak Gaussian fit to $e^-(D_2O)$ was optimized with the 220 cm^{-1} peak frequency fixed.

All of the librations observed for the solvated electron are clearly *downshifted*[31] relative to those of bulk water: H_2O has assignments 425−450, 530−590, and 715−766 cm^{-1}, respectively, for ν_{L1}, ν_{L2}, and ν_{L3}, and D_2O has assignments 305−350 and 535−570 cm^{-1}, respectively, for ν_{L1} and ν_{L3}.[30] Further evidence for an overall downshift of one or more librational bands follows from the separation of the peaks of the bend + librational combination band and the bend fundamental (see later text).

Resonance Raman spectra of the solvated electron in pure H_2O, D_2O, and five isotopic mixtures are presented in Figure 3. Spectra a−f were normalized to the average probe energy/pulse and electron concentration−length product of the $e^-(H_2O)$ experiment (spectra g), which were 109 μJ/pulse and 8.0 μM cm. An additional scaling factor of ~30% was required to increase spectrum b and decrease d so that the sum of the OH and OD stretch regions of the corresponding probe-only spectra (not shown) were roughly constant. The reason for this correction is possibly due to fluctuations in the jet.

(26) A wavelength-dependent correction compensating for the solvated electron's absorption of Raman emission from the bulk solution is unwarranted, since the off-resonant scattering originates primarily from the limited band spanning the OH and OD stretch regions.
(27) The probe-only OD/OH stretches integrated on a wavenumber axis without correction for the constant wavelength band-pass yield an OD stretch area that is 1.14-fold greater than the OH area. This ratio is within 2% of the 1.16 ratio of the OD/OH cross sections determined by 683 nm excitation of pure D_2O or H_2O in separate experiments employing a cuvette rather than the thin flowing jet.
(28) Jou, F. Y.; Freeman, G. R. *J. Phys. Chem.* **1979**, *83*, 2383.
(29) Bradforth, S. E. Personal communication.
(30) Walrafen, G. E. In *Water A Comprehensive Treatise*; Franks, F., Ed.; Plenum Press: New York, 1972; Vol. 1, p 151.
(31) Our previous impression (ref 22) that the libration appears slightly weighted towards a higher frequency in comparison with bulk water was based upon a partial view of the solvated electron librational band and resulted simply from the fact that the librations of the solvated electron are dramatically enhanced and also appear broadened relative to the nearly flat librational bands that are only weakly apparent in our off-resonance spectra of H_2O (see Figure 2).

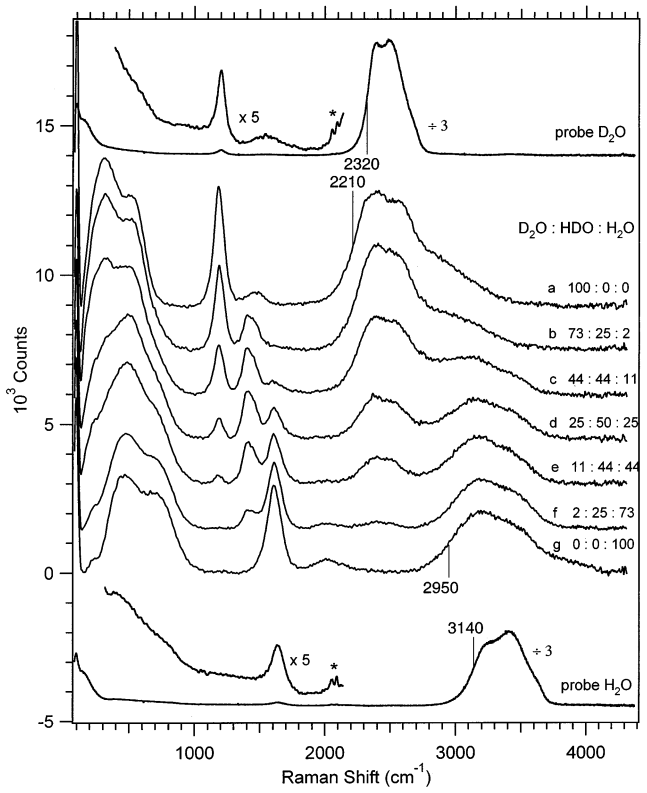

Figure 3. Resonance Raman spectra (a−g) of electrons in isotopic mixtures of D_2O/HOD/H_2O after the 70% subtraction of probe-only spectra and the removal of fluorescence backgrounds, as illustrated in Figure 1. Spectra a−f are offset in 1500 count intervals and normalized (see text) to the $e^-(H_2O)$ spectrum (g). Probe-only spectra of the ferrocyanide solutions in H_2O and D_2O are shown at bottom and top, scaled relative to the electron spectra by $^1/_3$. The libration and bend regions are also shown magnified 5-fold relative to the electron spectra. The weak doublet near 2100 cm^{-1} noted by * is due to ferricyanide.

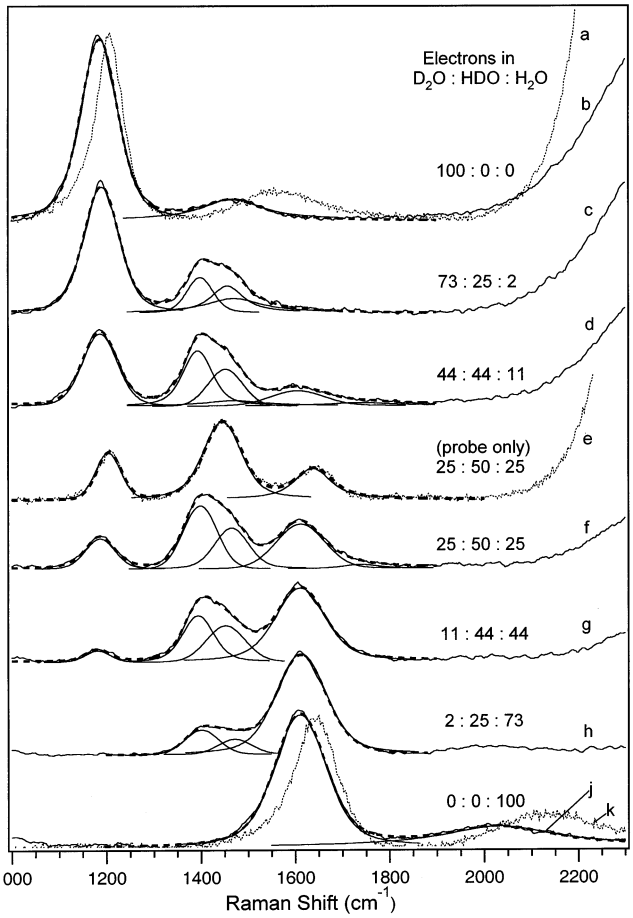

Figure 4. Magnified view of the 683-nm excited Raman bend region of the solvated electron (spectra b−d, f−j), shown as solid lines. The spectra of pure H_2O (a), D_2O (k), or an equimolar isotopic mixture (e) are presented by the dotted (•••) lines. Voigt peak fits to all solvated electron spectra, and to the 50:50 solvent mixture without electrons, are shown as solid symmetric peaks underlying the main spectra. The sums of the Voigt fits are shown as dashed (- - -) lines. The peak positions, widths, and areas of the component peaks are summarized in Table 1. The bend + librational combination bands centered at 2150 cm^{-1} (H_2O), 1580 cm^{-1} (D_2O), 2030 cm^{-1} $e^-(H_2O)$, and 1470 cm^{-1} $e^-(D_2O)$ were well fit in the isotopically pure samples. Minor peaks of fixed widths and at fixed positions of 1470 and 1750 cm^{-1} were added to the band fits of the solvated electron in isotopic mixtures to account for the combination band intensity due to $e^-(D_2O)$ and e^-(HOD), respectively.

A magnified view of the intramolecular bend and bend + librational combination band region is presented in Figure 4. The optimized peak positions, bandwidths, and areas are summarized in Table 1. The most unusual feature of the spectra is the definite appearance of a double peak for the HOD bending mode of the solvated electron. This splitting is apparent in the HOD bend of all isotopic mixtures of the electron and is highlighted by comparing the probe-only 25:50:25 mixture (spectrum e) to the corresponding solvated electron spectrum (spectrum f). This observation is profoundly important to the structural model of the solvated electron, as discussed later. Figure 4 also illustrates that the separation of the bend and bend + libration combination bands is 420 cm^{-1} for $e^-(H_2O)$ and 280 cm^{-1} for $e^-(D_2O)$. The ∼90 cm^{-1} reduction in band separation relative to the values in bulk liquid (510 cm^{-1} for H_2O and 370 cm^{-1} for D_2O) is partly attributed to a decrease in librational frequencies of the water molecules coupled to the electron.

Another unusual aspect of the electron−H_2O/HOD/D_2O bend peaks of Figure 4 is found in the relative intensities of the 25:50:25 mixture (spectrum f). The area of the $e^-(H_2O)$ peak is clearly greater despite the equal concentrations of H_2O and D_2O in the mixture and the nearly identical resonance Raman cross sections of these bands for the isotopically pure solvents. The Voigt fits to these bands (Table 1) indicate an ∼2-fold greater area for the $e^-(H_2O)$ bend relative to $e^-(D_2O)$. This area ratio is sensitive to the baseline fit to the lowest points of the Raman bend regions, as well as the inclusion of a minor bend + libration combination band for e^-(HOD) at 1750 cm^{-1} (see Figure 4). A more accurate determination of the relative enhancement is presented in Figure 5, where equal proportions of the $e^-(H_2O)$ and $e^-(D_2O)$ spectra are subtracted successively from the spectrum of the mixture. The stack plot guides the choice of the subtraction parameters that cause the complete disappearance of the $e^-(H_2O)$ or $e^-(D_2O)$ bend peaks in the mixed solvent spectrum. The ratio of the best subtraction parameters (2.2:1.4) indicates that the H_2O band is 1.6-fold more intense. Since we have shown that the separate cross sections for the subtracted components are nearly identical, this implies that there is a 1.6-fold preference of the solvated electrons for H_2O.

Table 1 summarizes the results of the band fitting to the mixed isotope spectra of the solvated electron which can be compared with fits to the probe-only solvent bands in Table 2. The

Table 1. Voigt Fits to Solvated Electron Water Bend

	center frequency (cm^{-1})				fwhm (cm^{-1})				area (au)			
$D_2O/HDO/H_2O$	D_2O	HDO		H_2O	D_2O	HDO		H_2O	D_2O	HDO		H_2O
100:0:0	1186				92				452			
73:25:2	1190	1399	1456		88	65	82		299	60	73	
44:44:11	1187	1394	1452	1605	86	74	86	<130[a]	156	114	72	46
25:50:25	1187	1399	1465	1612	73	84[b]	84[b]	119	53	120	85	121
11:44:44	1182	1394	1453	1611	62[a]	78	96	124	16	94	79	246
2:25:73		1401	1472	1612		83	83	125		46	28	329
0:0:100				1610				130				462

[a] The width of the $e^-(D_2O)$ bend for the 11% D_2O dilution is subject to error because of relatively a strong dependence on the baseline fit. Also, we are unable to fit the width of the $e^-(H_2O)$ band in 11% H_2O solution because of a strong overlap with the HOD combination band. [b] These values were fixed during the fit.

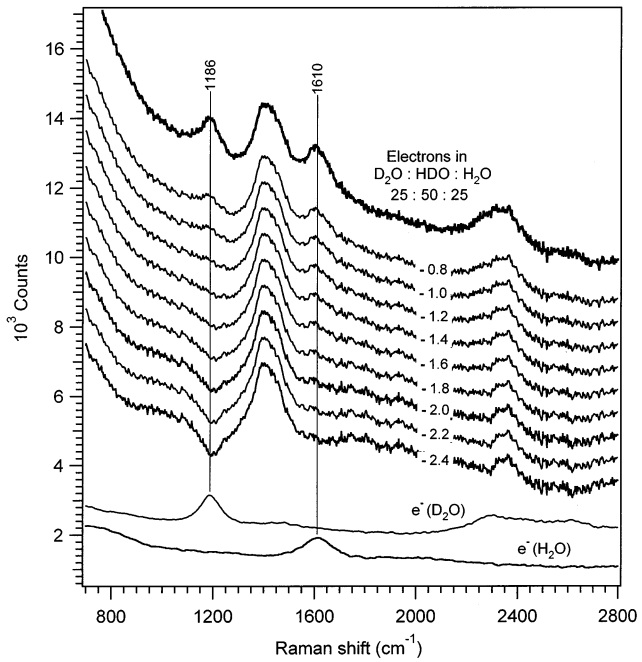

Figure 5. Resonance Raman spectrum of electrons in a 25:50:25 molar mixture of $D_2O/HDO/H_2O$ with fluorescence background unsubtracted (upper spectrum, vertically offset). Lower spectra are electron spectra in pure H_2O and D_2O, scaled relative to one another as described in Figure 1. Subtractions of equal amounts of the pure spectra from that of the mixture are shown with the subtraction factor indicated. The D_2O bend is completely removed with a subtraction coefficient of 1.4, whereas that of H_2O requires a subtraction of 2.0 or 2.2× the pure spectrum.

$e^-(D_2O)$ bend peak is ∼18 cm^{-1} downshifted relative to D_2O, and the $e^-(H_2O)$ bend is ∼30 cm^{-1} downshifted from H_2O. The average of the two e^-(HOD) bend peaks is ∼13−20 cm^{-1} downshifted from the HOD bend. The $e^-(D_2O)$ bandwidth decreases monotonically by ∼19 cm^{-1} upon dilution from 100% to 25% D_2O, whereas the $e^-(H_2O)$ bend shows ∼11 cm^{-1} narrowing for dilution of H_2O from 100% to 25%. By contrast, the narrowing of the bend bandwidths measured for spectra without electrons (Table 2) is approximately 2-fold greater for H_2O (∼14 cm^{-1}) than for D_2O (∼7 cm^{-1}) over the same dilution range 100%−25%. The central frequencies of $e^-(H_2O)$ and $e^-(D_2O)$ bends show a 5−7 cm^{-1} red shift for the most dilute (11%) solutions, whereas the probe-only peak frequencies of H_2O and D_2O show no significant deviation over the full dilution range.

The significant downshift in the low-frequency side of the OH stretch caused by the electron is apparent from comparing the low-frequency sides of the $e^-(H_2O)$ and $e^-(D_2O)$ with their respective probe-only counterparts (Figure 3). The red shift of the OH band is best quantified by the location of the half-maximum. This location is not strongly dependent upon the exact choice of probe-only subtraction, as shown in the successive subtractions of probe-only spectra in Figure 1, lower panel. The red shifts of the half-maxima are nearly 200 cm^{-1} for $e^-(H_2O)$ and ∼120 cm^{-1} for $e^-(D_2O)$ relative to the pure solvents.

On the high-frequency side of the OD stretch, there is clearly Raman scattering over the frequency range 2700−3300 cm^{-1}, which is beyond the highest frequency of the probe-only OD stretch (Figures 1 and 3a). The corresponding sloped decay past the high-frequency side of the OH stretch is not as obvious for electrons in H_2O (Figure 3, spectrum g) and is very dependent upon the baseline location (see Figure 1). The selected baseline leads to the appearance of Raman scattering out to nearly 4000 cm^{-1}. The blue shifted scattering is at higher frequencies than H_2O and D_2O fundamental stretches and is therefore assigned to combination bands of the stretches and librations.

The polarized spectra of the solvated electron are shown for $e^-(H_2O)$ and $e^-(D_2O)$ in Figure 6. The probe-only depolarization ratios acquired here at low power and with a thin flowing solution of 1.80 mM potassium ferrocyanide compare closely with literature spectra of pure water.[32−34] The solvated electron depolarization for the bend region is ∼1/3 for both $e^-(H_2O)$ and $e^-(D_2O)$, as expected for Raman scattering on resonance with a nondegenerate state.[35,36] In the librational region, the depolarization is ∼1/3 for $e^-(D_2O)$ but varies from 0.3 to 0.5 for $e^-(H_2O)$. The $e^-(H_2O)$ depolarization is considered more accurate because of the better fit to the baseline. Last, the depolarizations of the stretch scattering for $e^-(H_2O)$ and $e^-(D_2O)$ closely follow their probe-only counterparts.[33]

IV. Discussion

The results presented here reveal critical new information about the structure of the aqueous solvated electron. The vibrational frequencies observed for the isotopic mixtures indicate that the molecules nearest the electron reside in an asymmetric environment, consistent with electron−water binding through a single proton. Frequency shifts also reveal disruptions in the H-bond network beyond the first solvent shell

(32) Kabisch, G. *J. Mol. Struct.* **1981**, *77*, 219.
(33) Cunningham, K.; Lyons, P. A. *J. Chem. Phys.* **1973**, *59*, 2132.
(34) Benassi, P.; Mazzacurati, V.; Nardone, M.; Ricci, M. A.; Ruocco, G.; De Santis, A.; Frattini, R.; Sampoli, M. *Mol. Phys.* **1987**, *62*, 1467.
(35) Strommen, D. P. *J. Chem. Educ.* **1992**, *69*, 803.
(36) Hamaguchi, H. In *Advances in Infrared and Raman Spectroscopy*; Clark, R. J. H., Hester, R. E., Eds.; Wiley Heyden: London, 1985; Vol. 12, p 273.

Table 2. Voigt Fits to Water Bend

	center frequency (cm^{-1})			fwhm (cm^{-1})			area (au)		
$D_2O/HDO/H_2O$	D_2O	HDO	H_2O	D_2O	HDO	H_2O	D_2O	HDO	H_2O
100:0:0	1204			69			44		
73:25:2	1206	1460		69	108		29	9	
44:44:11	1203	1449	1640[b]	67	107	110[a,b]	19	17	4
25:50:25	1204	1445	1640	62	96	94	8	22	10
11:44:44	1205	1444	1642	59[a]	107	94	3	23	16
2:25:73		1448	1641		114	105		17	27
0:0:100			1640			108			42

[a] The width of the D_2O bend band at 11% dilution is subject to error because of a relatively strong dependence on the baseline fit. Also, we are unable to fit the width of the H_2O band in the 11% H_2O solution because of a strong overlap with the HOD combination band. [b] These values were fixed during the fit.

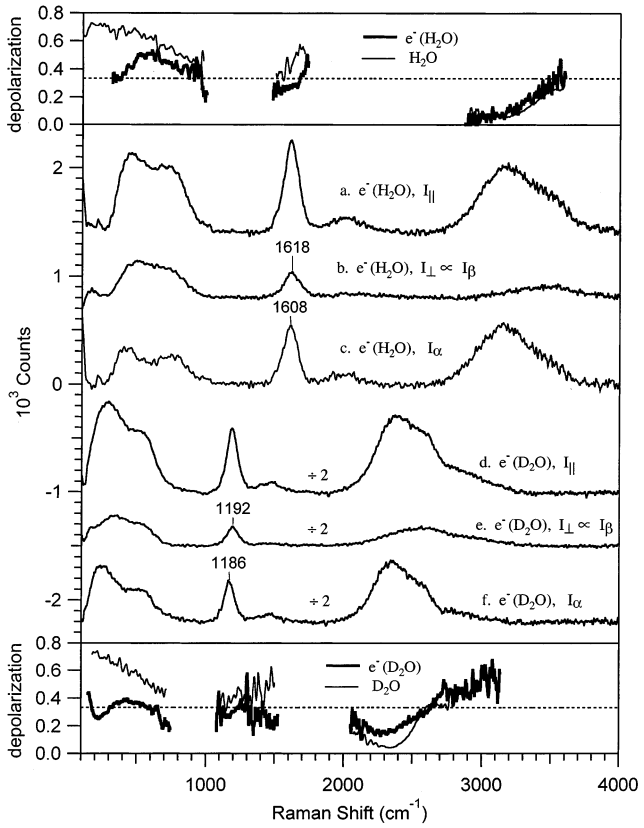

Figure 6. Polarized Raman spectra of electrons in H_2O and D_2O. (Middle panel) Spectra a and d are due to scattering $I_{||}$ parallel with the polarization of 683 nm excitation. Spectra b and e are due to perpendicular scattering $I_\perp$ which is proportional to the intensity of the anisotropic specta $I_\beta = {}^4/_3 I_\perp$. The isotropic spectra c and f are determined from ($I_\alpha = I_{||} - {}^4/_3 I_\perp$). The depolarization ratio $\rho = I_\perp/I_{||}$ of the solvated electron (bold lines) and the probe-only bulk 1.80 mM $K_4Fe(CN)_6$ solutions (fine lines) are shown for H_2O (upper panel) and D_2O (lower panel) in the libration, bend, and stretch regions.

and provide a structural insight into the exceptionally large entropy of electron hydration.[6,37,38] The preference of the electron for H_2O versus D_2O in mixed solvent is explained in terms of changes in zero-point energy upon binding and is consistent with the free energy of transfer of the electron from H_2O to D_2O calculated thermodynamically.[6]

Splitting of the HOD Bend Vibration. The doubled peak in the HOD bend of the solvated electron provides direct evidence about the structure and binding lifetime of the water solvent in this species. The water protons closest to the electron must be in an asymmetric environment; the difference between these two environments is quantified by the splitting of the bend. Our result rules out models that present water molecules dipole oriented toward the electron, since such a configuration results in a symmetric environment about both protons and would lead to a single HOD bend frequency. On the other hand, the "bond-oriented" structure suggested in spin−echo studies of the aqueous glass is consistent with our finding.[8] While the glass is a static structure, the interaction of the electron and nearest solvent molecules is obviously fluxional in nature. The ∼60 cm^{-1} separation of the two e^-(HOD) peaks implies a lifetime of the water−electron interaction of greater than ∼100 fs in the room temperature liquid.

Frequency Shifts of Bend, Stretch and Librations. The frequency shifts observed for the water intramolecular bend and stretch as well as intermolecular libration provide insights into the nature and strength of the electron−water interaction. It is most important to emphasize that the 200 (120) cm^{-1} downshifted OH (OD) stretch and the 30 (20) cm^{-1} downshifted H_2O (D_2O) bend frequencies are modest shifts (∼6% and ∼2%, respectively). Furthermore all bands of the resonance Raman spectrum of the aqueous solvated electron are directly correlated to fundamental or combination bands of the liquid. These two points underscore the essential conclusion that *the solvated electron is best considered a perturbation to the monomer units of liquid water*. Specifically our spectra provide no support for the H_3O hydronium model for the solvated electron[39] in either the radical[40] or charge-separated[41,42] forms, whose calculated vibrational frequencies bear little correspondence to the experimental spectra presented here.

The downshifted OH/OD stretch is perhaps the most important spectroscopic feature that specifically illuminates the nature of the electron−water bond. The cross section of this subsection of the enhanced stretch is approximately the same as that of the enhanced bend, and it is impossible to easily account for this intensity in terms of a bend overtone. Further evidence against its assignment as a bend overtone is the absence of any feature that corresponds to a HOD bend overtone. Therefore, we confidently assign the enhancement of the low-frequency wings of the OH (OD) stretches as downshifted OH (OD) modes.

(37) Han, P.; Bartels, D. M. *J. Phys. Chem.* **1990**, *94*, 7294.
(38) Schwarz, H. A. *J. Phys. Chem.* **1991**, *95*, 6697.
(39) This stimulating idea was first proposed in the seminal work of the late G. Wilse Robinson in: Hameka, H. F.; Robinson, G. W.; Marsden, C. J. *J. Phys. Chem.* **1987**, *91*, 3150.
(40) Muguet, F. 8th Electronic Computational Chemistry Conference. http://eccc8.cooper.edu (2002).
(41) Sobolewski, A. L.; Domcke, W. *Phys. Chem. Chem. Phys.* **2002**, *4*, 4.
(42) Sobolewski, A. L.; Domcke, W. *J. Phys. Chem. A* **2002**, *106*, 4158.

It is well established that the OH stretch frequency is correlated with H-bond strength.[43] Therefore, the significant downshift of the frequency at half intensity of the OH stretch provides clear evidence for a hydrogen bond between the solvated electron and the closest proton(s) that is slightly stronger than the average hydrogen bond in the bulk liquid. Our proposal of a strong electron−water bond is in agreement with recent ab initio calculations of electron−water clusters.[15,16,44] The electron−hydrogen interaction is found to provide stabilization comparable to a normal H bond.[16] The frequencies calculated for the largest ab initio cluster to date (electron +12 waters) indicate downshifts due to the electron that are 100−200 cm^{-1} relative to those of the neutral cluster.[16] The authors point out that the shifts would be greater at the MP2 level by up to 100 cm^{-1}, which leads to a prediction that agrees quantitatively with our finding.

The formation of a stable hydrogen bond to the electron is seemingly inconsistent with the 30(20) cm^{-1} *downshift* of the H_2O (D_2O) bend frequency *toward the gas-phase bend frequencies*. We proposed one solution to this inconsistency earlier in which weakly antibonding frontier molecular orbitals of water are partially occupied by the excess electron charge density.[21,22] This covalent interaction would slightly weaken all intramolecular modes and therefore lead to frequency downshifts. A second hypothesis is that protons opposite to the electron become poorer hydrogen bond donors to the 2nd shell molecules in comparison to the average donating H bond in the bulk liquid. The two hypotheses could be closely linked, since the extent of covalent interaction between the electron and nearest water molecules is likely a determining factor in the H-bond donating ability of the outlying proton. However, the explanation that focuses only upon the changes in hydrogen bonding is preferable, because it draws attention to the principle *result* of the electron perturbation without presupposing whether the fundamental cause is due to a covalent or ionic interaction between the electron and nearest water molecules.

The shifts in the bend frequencies of H_2O, D_2O, and HOD are readily explained in terms of the changes in hydrogen bonding to molecules in the first solvent shell. The downshifts of the $e^-(H_2O)$ and $e^-(D_2O)$ bend frequencies are evidence that the weakened interactions to the 2nd solvent shell predominate over the strengthened H bond to the electron. The low-frequency component of the HOD bend is strongly downshifted (∼48 cm^{-1}) relative to the bulk liquid bend at 1445 cm^{-1} and is even downshifted below the gas-phase HOD frequency of 1402 cm^{-1}.[45] Furthermore, the other component in the e^-(HOD) bend is upshifted from the liquid value by ∼12 cm^{-1}. For HOD bound to the electron through the H atom, it is reasonable to propose that strong electron−hydrogen interaction and weak binding to D leads to an HOD bend normal mode that consists of a relatively greater contribution from the motion of deuterium compared with that of the HOD bend in the bulk liquid (or gas phase), thus lowering the frequency of this mode to 1397 cm^{-1}. For HOD bound to the excess electron through D, the HOD bend motion then consists of greater H motion and is therefore slightly upshifted (∼12 cm^{-1}). Thus, we see that the asymmetric H-bond environment accounts for the HOD bend split.

The frequency downshifts of the librations of the water molecules surrounding the electron are consistent with the overall downshifts of the bend frequency and as a whole reveal disruptions between the 1st and 2nd shell molecules. The connection between the downshifted librations and bend follows from the explanation[46] for the higher bend frequency in the liquid phase relative to the gas-phase values 1595 (1178) cm^{-1} for H_2O (D_2O): The same H-bond forces that hinder the water rotations in the liquid cause a force tangential to the OH axis and therefore an upshift in the bend frequency. Our observation of significant downshifts of both the bend and the librations of the solvated electron indicates that the molecules in the first solvent shell experience weaker forces tangential to the OH bond axis than their counterparts in the bulk liquid. The two contributing factors for the decreased tangential force include both disruption of H bonds between 1st and 2nd solvent shells, as well as the likely possibility that the diffuse solvated electron provides less resistance to rotation than a hydrogen bond to a classical anion such as a halide.

The model presented above invites a second look at the origin of the high-frequency scattering > 3400 cm^{-1} (OH) and > 2500 cm^{-1} (OD) from the solvated electron (Figure 4). We have attributed[22] the intensity at frequencies > 3760 (2790) cm^{-1} for H_2O (D_2O) to combination bands of the stretch plus librations, since this part of the scattering is beyond the highest conceivable stretching fundamental frequencies.[45] The spectra presented in Figure 4 also indicate significant scattering from 3400 to 3700 cm^{-1} for $e^-(H_2O)$ and from 2500 to 2700 cm^{-1} for $e^-(D_2O)$. In the pure bulk solvents, this scattering is attributed to OH (OD) oscillators of asymmetrically bound water molecules that have relatively weak or broken H bonds.[47] Similarly, we suggest that this intensity in the case of the solvated electron may derive from resonantly enhanced OH (OD) oscillators that are oriented away from the electron and toward the 2nd solvent shell, where they experience weak hydrogen bonding. In summary, it is possible that Raman scattering on the high-frequency side of the OH (OD) stretch derives intensity from both the combination band and OH (OD) bonds that are weakly hydrogen bonded.

Equilibrium Isotope Effect. Our measurement of a 1.6-fold preference of the solvated electron for H_2O in the 25:50:25 mixture of H_2O/HOD/D_2O is an example of isotope fractionation by an ion.[48] Specifically, the equilibrium constant $K_{eq} = 1.6$ quantifies the thermodynamic preference for H_2O in the complexes by $e^-(H_2O)_x(D_2O)_y(HOD)_z$, where the total number of water molecules contributing to the resonantly enhanced Raman signal is the sum $x + y + z$. For each member of the set of complexes contributing to the H_2O resonant bend intensity in the 25:50:25 mixture of H_2O/HOD/D_2O, there exists a companion species that contributes to the D_2O bend signal in exactly the same statistical proportion; the two species are stoichiometrically related by the exchange of a single H_2O for D_2O. The generalization of this fact leads to the conclusion that the equilibrium constant $K_{eq} = 1.6$ ($\Delta G = -0.28$ kcal/mol)

(43) Pimentel, G. C.; McClellan, A. L. *The Hydrogen Bond*; Freeman: San Francisco, CA, 1960.
(44) Kim, K. S.; Park, I.; Lee, S.; Cho, K.; Lee, J. Y.; Kim, J.; Joannopoulos, J. D. *Phys. Rev. Lett.* **1996**, *76*, 956.
(45) Herzberg, G. *Molecular Spectra and Molecular Structure II. Infrared and Raman Spectra of Polyatomic Molecules*; Krieger Publishing Company: Malabar, FL, 1945.
(46) Cross, P. C.; Burnham, J.; Leighton, P. A. *J. Am. Chem. Soc.* **1937**, *59*, 1134.
(47) Scherer, J. R. In *Advances in Infrared and Raman Spectroscopy*; Clark, R. J. H., Hester, R. E., Eds.; Heyden: London, 1978; Vol. 5, p 149.
(48) Newton, M. D.; Friedman, H. L. *J. Chem. Phys.* **1985**, *83*, 5210.

quantifies the free energy of exchange of a single D_2O in the electron−water complex for a single H_2O, averaged over all stoichiometric species probed.

The simplest explanation for this equilibrium isotope effect is based upon the observed downshifts in OH (OD) stretch frequencies. The explanation of a normal isotope effect in general invokes the zero-point energy difference between the bound and unbound ligands. A larger separation of the zero-point energy levels for a tighter bond leads to the conclusion that the heavier isotope energetically prefers the tighter bond. We clearly observe upon binding that the OH (OD) stretch frequency downshifts 200 (120) cm^{-1}. Thus, it is expected that the equilibrium below is shifted to the right:

$$e^-(H_2O)_x(D_2O)_y(HOD)_z + H_2O \rightarrow e^-(H_2O)_{x+1}(D_2O)_{y-1}(HOD)_z + D_2O$$

Interestingly, the difference in the ZPE of products and reactants for the reaction derived only from the differences in the low-frequency stretches leads to an estimate of 50 cm^{-1}/molecule free energy in favor of the products. The ΔG determined from the equilibrium constant above (−0.28 kcal/mol) corresponds to 100 cm^{-1}/bound molecule. This qualitative agreement indicates that the traditional explanation for the normal isotope effect holds true for the equilibrium reaction here.

Our measurement of a preference of the electron for H_2O in a equimolar mixture implies that the process of transferring an electron from pure H_2O to D_2O is energetically unfavorable. The qualitative trend of greater stability in H_2O is consistent with the sign of the free energy of transfer from H_2O to D_2O ($\Delta G_{trans} = +1.3 \pm 1.1$ kJ/mol) calculated from a Born−Haber cycle.[6]

Polarized Spectra. The average value of the depolarization ρ across the bend mode (Figure 6) is $\sim 1/3$ for both $e^-(H_2O)$ and $e^-(D_2O)$, which is consistent with resonant excitation of a nondegenerate state. This result is compatible with disparate models of the electronic absorption of the solvated electron, which is interpreted either as a single homogeneously broadened band[49] or as three subbands that are largely split by inhomogeneous (site) broadening.[50] On the other hand, the depolarization of both the OH and OD stretches appear to vary significantly across the band and are clearly less than $1/3$ on the low-frequency side. Additionally, the depolarization of the libration of $e^-(H_2O)$ is significantly greater than $1/3$ over most of the band. These significant deviations from $1/3$ and the variation across the band are clearly incompatible with a resonant transition to a single nondegenerate state.[35] Our resonance Raman intensity analysis suggests that the homogeneous broadening of the solvated electron electronic transition is ~2-fold greater than the inhomogeneous broadening[22] which leads to the intriguing possibility that strongly overlapped subbands may cause the mode-specific variation from $1/3$.[36,51,52]

The isotropic I_α linear combination of polarized spectra is presented in Figure 6 in comparison with the anisotropic spectrum I_β.[53] The isotropic and anisotropic OH/OD stretch peaks of our resonance Raman spectra are separated far too much to be explained in terms of the classical Raman noncoincidence effect because of the intermolecular coupling of transition dipole moments.[54,55] However, the noncoincidence of the electron−water resonance Raman bend peaks are ~10 cm^{-1} for $e^-(H_2O)$ and 6 cm^{-1} for $e^-(D_2O)$ and are likely due to intermolecular coupling because these values are comparable to the Raman noncoincidence of the pure liquid bend (19 cm^{-1} for H_2O and 7 cm^{-1} for D_2O) whose origin in intermolecular coupling has been well established.[32] Moreover, the specific value of the noncoincidence for the solvated electron might provide an important constraint on the orientation and number of solvent molecules in the 1st solvent shell, as suggested for a recent calculation of the Raman noncoincidence of electrons solvated in methanol.[56]

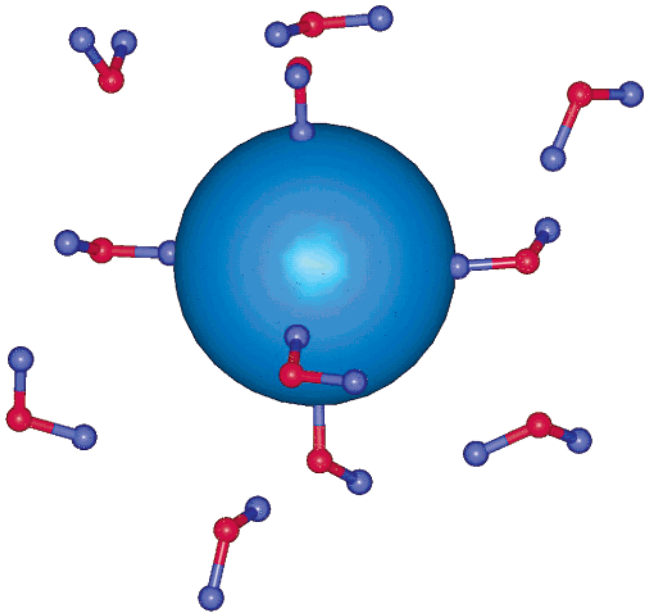

Figure 7. Schematic representation of molecules in the first and second coordination shells around the solvated electron. First shell molecules are shown hydrogen bonded to the electron. Hydrogen bonds between molecules of first and second shells are disrupted. Although shown as an octahedral field,[8] our data do not define the number of surrounding water molecules or the symmetry.

Relationship to Bulk Thermodynamic Measurements. We now reconcile our structure of the solvated electron with the fact that the electron is the only ion with a positive entropy of hydration and is therefore considered "a champion structure breaker".[6,37] We propose that the 1st solvent shell is in fact highly ordered, as illustrated in Figure 7. This is not inconsistent with the thermodynamics because much of the disorder is likely found in the 2nd shell. Our model is closely related to a picture of anion solvation proposed by Frank and Wen,[57] in which the regions around an anion are divided into zones: In the zone closest to the anion, water molecules are highly oriented; in

(49) Baltuska, A. Hydrated Electron Dynamics Explored with 5-fs Optical Pulses, University of Groningen, 2000.
(50) Schwartz, B. J.; Rossky, P. J. *J. Chem. Phys.* **1994**, *101*, 6902.
(51) Shang, Q.; Hudson, B. S. *Chem. Phys. Lett.* **1991**, *183*, 63.
(52) Harhay, G. P.; Hudson, B. S. *J. Phys. Chem. A* **2000**, *104*, 681.

(53) The classic analysis of the noncoincidence effect is developed for off-resonance Raman scattering, in which only totally symmetric modes contribute to isotropic spectra $I_\alpha = I_{||} - 4/3 I_\perp$. In the resonance Raman spectra presented here, all enhanced intramolecular modes are thought to be due to displacements along totally symmetric normal modes in the local C_{2v} point group. However, intermolecular coupling leads to dispersion of the various phases of these totally symmetric modes that are perhaps best characterized by the anisotropic and isotropic spectra in analogy to the off-resonance treatment.
(54) Wang, C. H.; McHale, J. L. *J. Chem. Phys* **1980**, *72*, 4039.
(55) Logan, D. E. *Chem. Phys.* **1989**, *131*, 199.
(56) Torii, H. *J. Phys. Chem. A* **1999**, *103*, 2843.
(57) Frank, H. S.; Wen, W. *Discuss. Faraday Soc.* **1957**, *24*, 133.

the zone farthest from the anion, the structure of bulk water is retained. Between these regions, the structure of water is broken down, thus giving rise to a "fault zone".[58]

Comparison with Spectra of Electrolyte Solutions. The Raman and IR spectra of aqueous electrolyte solutions[59−62] can be cautiously compared with our spectra of the aqueous solvated electron. The resonant probe employed here selectively enhances scattering from a small number of water molecules in the vicinity of dilute electrons, in contrast with off-resonance Raman and IR studies which probe highly concentrated electrolyte solutions. The intensity of the intramolecular water bend of aqueous electrolytes is strongly enhanced relative to pure water,[63] which echos the resonance enhancement observed here. The bend frequency of concentrated aqueous halide solutions shows no shift from the pure liquid[59] with the exception of a small (∼10 cm^{-1}) downshift observed for concentrated iodide.[64] It is possible that this downshift has a similar origin to the larger downshift observed here. The OH and OD stretch regions of concentrated halide solutions show primarily frequency upshifts, which are evidence for structure-breaking effects that are also found for the aqueous solvated electron.

Structure of the Solvated Electron. The Raman structural data presented here provide powerful constraints on models for the structure of the solvated electron. Our data are *inconsistent* with an electron associated primarily with a single water monomer $(H_2O)^-_{aq}$.[65] If the solvated monomer anion was an accurate representation, we would expect that the resonance Raman enhancements are primarily due to the central water anion, which must show evidence of asymmetric binding to its surroundings presumably via one strong and one weak hydrogen bond. However, the formation of a strong hydrogen bond by a negatively charged species is not plausible without a large degree of charge transfer to the surrounding solvent molecules, contradictory to the initial hypothesis.

On the other hand, our data are consistent with the model of a "solvated anion cluster", in which the Raman scattering derives from an electron bound to more than one water molecule. The solvated electron in association with these water molecules must result in the following: (1) resonantly enhanced OH bonds that are hydrogen bonded asymmetrically, (2) at least one resonantly enhanced OH bond that forms an exceptionally strong donor hydrogen bond to the electron or possibly to oxygen, and (3) weak or disrupted H bonds. It is clear that the cavity model fits all of these requirements and is a special case of a solvated anion cluster in which a comparatively large number of waters are directly hydrogen bonded to the electron.

V. Conclusion

Our data show unequivocally that the species participating in the resonance Raman scattering of the aqueous solvated electron are *perturbed water monomers*. Two or more of these water molecules are Franck−Condon coupled to the electron, and their strong interaction with the electron leads to weakened hydrogen bonds to the bulk solvent. The frequency splitting of the resonantly enhanced HOD bend reveals the bond-oriented structure of water molecules nearest the electron. These conclusions provide an enhanced molecular picture of the prevailing cavity model of the aqueous solvated electron.

Acknowledgment. We thank David McCamant and Judy Kim for many helpful discussions and Ziad Ganim for providing Figure 7. Discussions with Herb Strauss, Avram Bromberg, Jim Scherer, and Steve Bradforth, and references brought to our attention by Ilya Shkrob and Takatoshi Ichino are also much appreciated. We thank Burt Mooney of Molectron Inc. for use of the power meter and Meadowlark Optics for donation of the VersaLight polarizer. This work was supported by a grant from the NSF (CHE-9801651) and by the Mathies Royalty Fund.

JA021134A

(58) Wicke, E. *Angew. Chem., Int. Ed. Engl.* **1966**, *5*, 106.
(59) Lilley, T. H. In *Water*; Franks, F., Ed.; Plenum Press: New York, 1973; Vol. 3, p 265.
(60) Verrall, R. E. In *Water*; Franks, F., Ed.; Plenum Press: New York, 1973; Vol. 3, p 211.
(61) Irish, D. E.; Brooker, M. H. In *Advances in Infrared and Raman Spectroscopy*; Clark, R. J. H., Hester, R. E., Eds.; Heyden: London, 1976; Vol. 2, p 212.
(62) Brooker, M. H. In *The Chemical Physics of Solvation, Part B Spectroscopy of Solvation*; Dogonadze, R. R., Kalman, E., Kornyshev, A. A., Ulstrup, J., Eds.; Elsevier: Amsterdam, 1986; Vol. 38, p 119.
(63) Schultz, J. W.; Hornig, D. F. *J. Phys. Chem.* **1961**, *65*, 2131.
(64) Weston, R. E., Jr. *Spectrochim. Acta* **1962**, *18*, 1257.
(65) Tuttle, T. R., Jr.; Golden, S. *J. Phys. Chem.* **1991**, *95*, 5725.